Acta Crystallographica Section D
Biological Crystallography
ISSN 0907-4449

Solving the structure of *Escherichia coli* elongation factor Tu using a twinned data set

Susan E. Heffron,[a] Rhonda Moeller[b] and Frances Jurnak[a]*

[a]University of California, Irvine, USA, and [b]CRG Laboratories Inc., Torrance, CA 90501, USA

Correspondence e-mail: jurnak@uci.edu

Received 15 September 2005
Accepted 1 February 2006

PDB Reference: *Escherichia coli* elongation factor Tu, 2fx3, r12fx3sf.

Escherichia coli elongation factor Tu–GDP (EF-Tu–GDP) was crystallized in the presence of novel inhibitors. The only crystals which could be grown were epitaxially as well as merohedrally twinned, highly mosaic and diffracted to a resolution of 3.4 Å in space group $P3_121$, with unit-cell parameters $a = b = 69.55$, $c = 169.44$ Å, $\alpha = \beta = 90$, $\gamma = 120^\circ$. To determine whether an inhibitor was present in the crystal, a poor-quality X-ray diffraction data set had to be processed. The three-dimensional structure was ultimately solved and the original question answered. The results also reveal a new type of dimer packing for EF-Tu–GDP.

1. Introduction

Elongation factor Tu is an essential component of the bacterial protein biosynthetic pathway. Its primary function is to recognize and transport non-initiator aminoacyl-tRNA to the A site of ribosomes during the elongation cycle (Abel & Jurnak, 1996). EF-Tu is a three-domain protein that undergoes a series of conformational changes as it binds to its substrates, including GDP (Abel *et al.*, 1996; Polekhina *et al.*, 1996), GTP (Berchtold *et al.*, 1993; Kjeldgaard *et al.*, 1993), aminoacyl-tRNA (Nissen *et al.*, 1995) and another elongation factor, EF-Ts (Kawashima *et al.*, 1996). A number of antibiotics target EF-Tu, blocking the necessary conformational changes or competing for the substrate-binding sites (Parmeggiani & Swart, 1985; Cetin *et al.*, 1996; Anborgh *et al.*, 2004; Deibel *et al.*, 2004; Jayasekera *et al.*, 2005). The binding sites of three antibiotics, the thiazolyl peptide GE2270A (Heffron & Jurnak, 2000) and auredox (Vogeley *et al.*, 2001) and enacyloxin IIa (Parmeggiani *et al.*, 2006), have been determined by X-ray diffraction analyses. The GE2270A-binding site lies in the second domain of EF-Tu and partly overlaps with the binding site of aminoacyl-tRNA. Although GE2270A has insufficient aqueous solubility to be a good antibiotic, the GE2270A-binding site on EF-Tu has excellent features for a druggable pocket, including volume, shape and surface polarity (An *et al.*, 2004).

Virtual ligand-screening methods (Cavasotto *et al.*, 2003) had been used to identify small soluble compounds that are likely to bind in the GE2270A site on EF-Tu–MgGDP. Crystals of EF-Tu were grown in the presence of compounds which inhibited protein synthesis in separate assays. Most crystals diffracted very poorly, but one diffraction data set was collected from a crystal that was highly mosaic, epitaxially and merohedrally twinned and diffracted to a resolution of 3.4 Å. To determine whether an inhibitor was present in the crystal, a poor-quality X-ray diffraction data set had to be processed. The three-dimensional structure was ultimately solved and the novel features of the structural results are also presented.

2. Experimental methods

2.1. Crystallization and data collection

EF-Tu–MgGDP (MW 43 643 Da) was purified from *Escherichia coli* B cells as described previously (Louie *et al.*, 1984). Compound 1013-0135 (MW 389 Da) was obtained as a gift from Chemical Diversity Laboratories Inc. (San Diego, CA, USA). Unless otherwise noted, all reagents were purchased from Sigma (St Louis, MO, USA). Crystals were grown within 3 d at 293 K by the sitting-drop vapor-diffusion method using a reservoir containing 0.5%(*w*/*v*) PEG 3350. The protein droplet contained a solution of 0.45 m*M* EF-Tu in 50 m*M* Tris pH 7.8, 10 m*M* GDP, 10 m*M* magnesium chloride, 1.34 m*M* compound 1013-0135, 0.5% PEG 3350, 5.5 m*M* ammonium acetate and 2.7 m*M* ammonium citrate. For data collection, a crystal with approximate dimensions of 0.1 × 0.1 × 0.04 mm was swiped through 40% glycerol and flash-frozen at 95 K. Using an oscillation angle of 1°, 154 X-ray diffraction images were measured from a single crystal at the Advanced Light Source in Berkeley, beamline 5.0.2, using a wavelength of 1.033 Å.

2.2. Data reduction

2.2.1. Autoindexing, scaling and merging. After removing reflections due to epitaxial twinning from the autoindexing reflection set, autoindexing and data integration were carried out using *MOSFLM* (Steller *et al.*, 1997). The initial beam center, which was erroneously provided by the beamline operators, was determined by reiterative autoindexing and later determined to be consistent with the coordinates calculated by the program *LABELIT* (Sauter *et al.*, 2004) using the server at http://adder.lbl.gov/labelit. Reflections were scaled and merged with *SCALA* (Evans, 1997) using the *CCP*4 graphical user interface *CCP*4*i* (Potterton *et al.*, 2003). Intensities were converted to structure-factor amplitudes using *TRUNCATE* (French & Wilson, 1978).

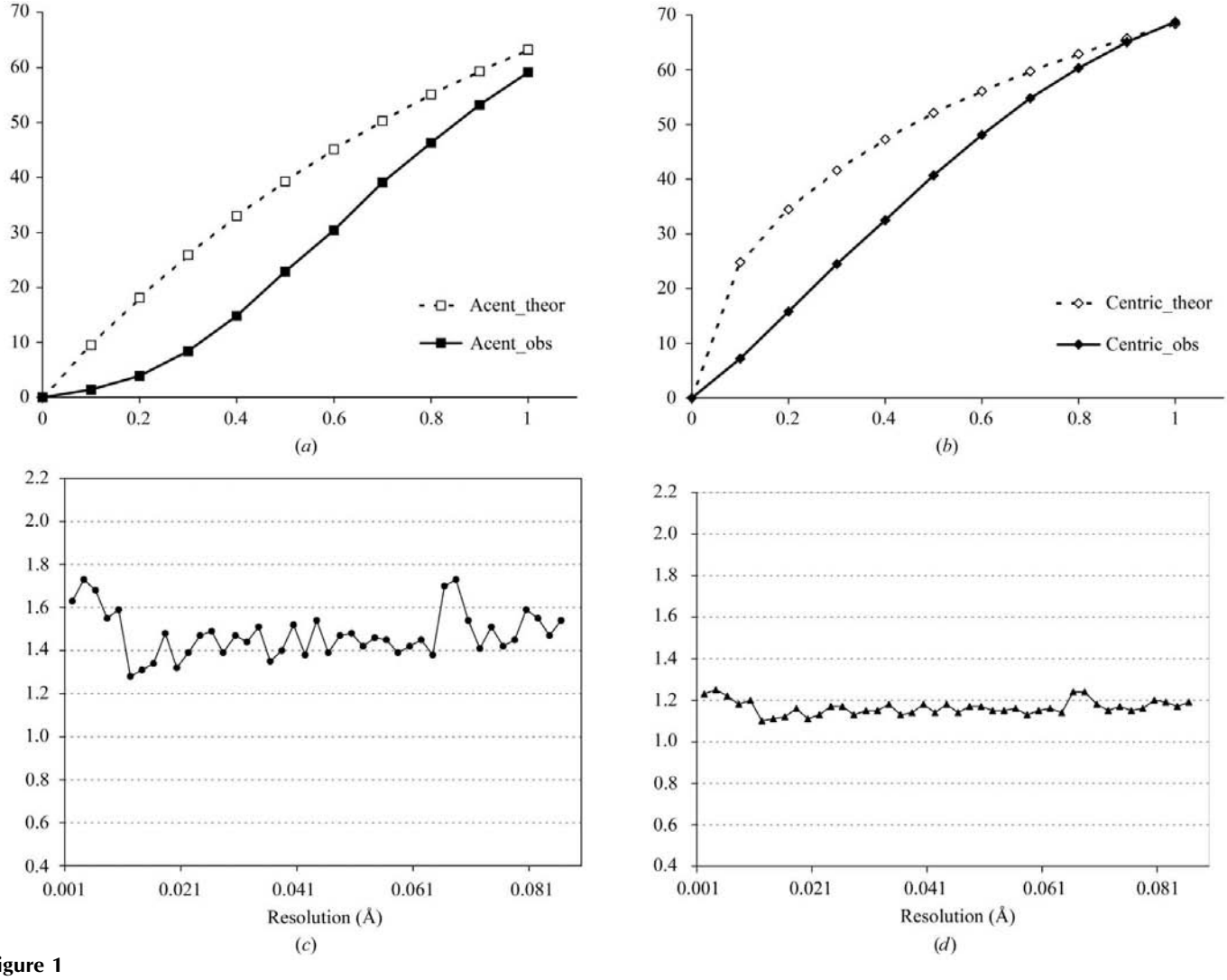

Figure 1
Plots using data from *TRUNCATE* that indicate that the crystal is merohedrally twinned. (*a*) and (*b*) Cumulative intensity distribution plots for acentric and centric data. In each case, the curve of the actual data was shifted to the right of the theoretical curve, indicating that the data was twinned. (*c*) Plot of the second moment of I ($\langle I^2\rangle/\langle I\rangle^2$), calculated in thin resolution shells. The expected value for untwinned data is 2.0 and that for a perfect twin is 1.5. (*d*) Plot of the third moment of E, calculated in thin resolution shells. The expected value for untwinned data is 1.329 and that for a perfect twin is 1.175.

Table 1
Data statistics in various possible space groups.

The resolution range was 3.40–60.20 Å. Values in parentheses are for the highest resolution bin (3.40–3.58 Å).

	*P*3	*P*6	*P*321	*P*312
Molecules per ASU	2	1	1	1
No. of reflections measured	41398	41251	41348	41248
No. of unique reflections	10895	5779	6312	6117
Completeness (%)	86.3 (80.1)	90.6 (85.8)	90.2 (84.9)	91.0 (86.6)
$R_{\rm sym}$†	0.160 (0.448)	0.240 (0.543)	0.174 (0.480)	0.239 (0.537)
$R_{\rm meas}$‡	0.184 (0.518)	0.258 (0.585)	0.188 (0.519)	0.257 (0.580)
$I/\sigma(I)$	3.4 (1.6)	2.3 (1.3)	3.2 (1.5)	2.3 (1.4)
Multiplicity	3.8 (3.9)	7.1 (7.3)	6.6 (6.9)	6.7 (6.9)

† $R_{\rm sym} = \sum(|I - \langle I\rangle|)/\sum I$. ‡ $R_{\rm meas}$ is a redundancy-independent $R_{\rm merge}$ (Diederichs & Karplus, 1997).

2.2.2. Space-group determination. Initially, the data set was processed in space group *P*3. The space-group choices were narrowed from 21 possibilities by reindexing the data in various space groups and then comparing the data statistics after scaling (Table 1). To reindex the unmerged data file from *P*3 to other primitive trigonal or hexagonal space groups (*P*3, *P*6, *P*321 and *P*312), the *CCP*4 programs *REINDEX* and *SORTMTZ* (Collaborative Computational Project, Number 4, 1994) were used. The final space-group determination was made by searching for molecular-replacement solutions in three related space groups.

2.2.3. Merohedral twinning detection. To detect merohedral twinning, the cumulative intensity distribution plots from *TRUNCATE* were examined, as well as the plots of the second, third and fourth moments of *E* or *I*. The twin fraction α was calculated using the *Merohedral Crystal Twinning Server* (Yeates, 1997), available at http://nihserver.mbi.ucla.edu/Twinning.

2.3. Molecular replacement

The search model for molecular replacement was the structure of EF-Tu taken from the complex of EF-Tu–MgGDP with the thiazolyl peptide antibiotic GE2270A (PDB code 1d8t; Heffron & Jurnak, 2000). Only atomic coordinates from chain *A*, without the antibiotic, were used in the search model. The structure was phased by molecular-replacement methods using the 'autosearch' mode of the program *PHASER* (Read, 2001; Storoni *et al.*, 2004) using the *CCP*4 graphical user interface *CCP*4*i*. Alternative space groups were tested during molecular replacement using data between 3.4 and 60 Å without detwinning the data.

2.4. Refinement and model building

Crystallographic refinement was carried out in *CNS* (Brünger *et al.*, 1998) using specialized task files for use with hemihedrally twinned data throughout the process, including map generation. The task file `make_cv_twin.inp` was used to select 9% of the reflections to be set aside as the cross-validation set during refinement, ensuring that pairs of twin-related reflections were designated as being in the same set, either the working set or the test set. The initial refinement included rigid-body refinement with each of the three domains of EF-Tu considered as a separate rigid body, followed by conjugate-gradient minimization. $\sigma_{\rm A}$-weighted electron-density maps (Read, 1986) were generated with *CNS* and reformatted using *MAPMAN* (Kleywegt & Jones, 1996). Manual model adjustment was performed using the program *O* (Jones *et al.*, 1990). After several rounds of refinement and model adjustment, *PROCHECK* (Laskowski *et al.*, 1993) was used to evaluate the quality of the final model.

3. Results and discussion

3.1. Detection of merohedral twinning

The output from *TRUNCATE* indicated that the diffraction data originated from a merohedrally twinned crystal. The plot of cumulative intensity distribution revealed that the curves for observed acentric and centric data were both shifted to lower values than the theoretical curves, indicating that twinning was present. Also, the curve for acentric observed data was sigmoidal, which was also consistent with twinned data. The intensity distribution curves are shown in Figs. 1(*a*) and 1(*b*). In addition, the values of the second moment of the intensity (I) and third moment of the normalized intensity (E) for acentric data were typical of twinned data, as shown in Figs. 1(*c*) and 1(*d*), plotted in thin resolution shells. The mean value of the second moment of I was 1.48, which is in close agreement with the expected value for perfectly twinned data of 1.5, compared with the expected value of 2.0 for untwinned data. The mean value of the third moment of E was 1.16, which is in close agreement with the expected value of 1.175 for perfectly twinned data, compared with the expected value of 1.329 for untwinned data. The small deviation from expected values for perfectly twinned data served as motivation to calculate the partial twin fraction of 0.294 for this crystal using the *Merohedral Crystal Twinning Server* (Yeates, 1997). The twin operation was $-h, -k, l$, indicating a twofold relationship parallel to the *c* axis.

3.2. Molecular-replacement results

The space-group choices were narrowed from the original 21 possibilities by reindexing the data in various space groups and then comparing the data statistics after scaling. Molecular replacement was used for phasing and also as an effective means of determining the final space-group assignment from the remaining three possibilities, *P*321, $P3_121$ or $P3_221$. The program *PHASER* ran molecular-replacement searches in alternative space groups and the best solution was found in space group $P3_121$, with a log-likelihood gain of 60.85. A summary of the molecular-replacement searches is shown in Table 2. Space group $P3_121$ with unit-cell parameters $a = b = 69.55$, $c = 169.44$ Å, $\alpha = \beta = 90$, $\gamma = 120^\circ$ was subsequently confirmed by the successful structural refinement.

Table 2
Summary of molecular-replacement searches.

	Euler angles			*X* trans	*Y* trans	*Z* trans	Rotational score	Translational score	LLG†
*P*3									
Molecule 1	—	—	—	No solutions without clashes			—	—	—
Molecule 2	—	—	—				—	—	—
$P3_1$									
Molecule 1	335.9	26.1	43.7	−1.226	−0.524	−0.322	27	61	82.6
Molecule 2‡	148.2	153.5	226.0	−0.81	−1.88	0.07	82	−32	45.2
$P3_2$									
Molecule 1	268.7	154.4	226.1	1.26	0.68	0.33	27	−11	−4.2
Molecule 2	—	—	—	—	—	—	—	—	—
*P*321	—	—	—	No solutions without clashes			—	—	—
$P3_121$	334.2	26.3	44.6	−1.56	−0.17	−0.20	21	−49	60.8
$P3_221$	267.4	154.0	225.0	1.43	0.40	0.36	21	−305	−251.9

† Log-likelihood gain of refined solution from *PHASER*. ‡ Search solution of second molecule with first molecule fixed.

3.3. Refinement and structural results

Refinement with the twinned-data version of *CNS* resulted in interpretable maps and acceptable *R* factors. Unfortunately, there was no electron density for the inhibitor in the binding site in domain 2, nor anywhere else on the protein. The GE2270A-binding site was in fact blocked by neighboring molecules in this crystal form, as shown in Fig. 2, and was thus unavailable to a potential inhibitor. The final model included residues 7–393 of the protein, one GDP molecule, one Mg^{2+} ion and four water molecules. The final R_{work} was 0.20 and R_{free} was 0.26. The overall quality of the model was indicated by a root-mean-square deviation of 0.01 Å from ideal bonds and 1.73° from ideal angles. Four residues were in the disallowed region of the Ramachandran plot, including Thr8, Ser221, Ile247 and Arg333, which is consistent with other EF-Tu structures.

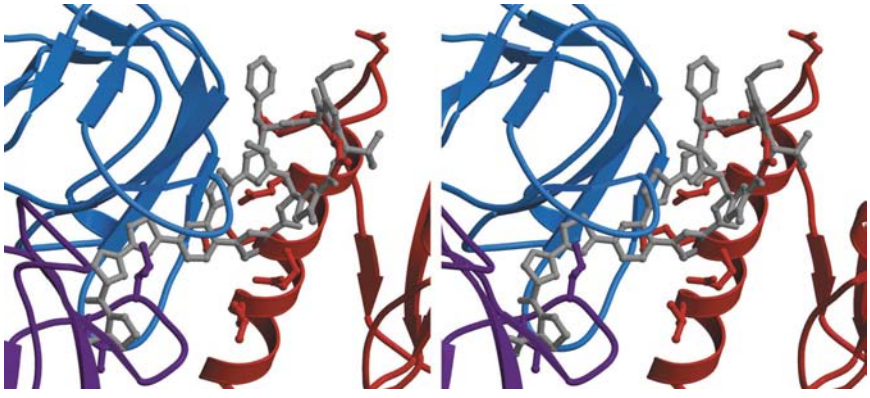

Figure 2
Stereo image of a close-up of the GE2270A-binding site in the second domain of EF-Tu, illustrating that crystal packing blocks the binding site. EF-Tu is shown as a ribbon, with one molecule in blue, the second in red and the third neighboring molecule in purple. GDP is represented by an orange or green stick model and Mg^{2+} ion by an orange or green sphere. To illustrate that the antibiotic binding site is unavailable as a consequence of steric clashes with crystal-packing interactions, a grey stick representation of GE2270A has been placed in its normal binding site in domain 2 of the blue copy of EF-Tu. The side chains from domain 1 of a neighboring EF-Tu, which protrude into the GE2270A-binding site, are shown in red stick representation. The side chains from domain 2 of another neighboring EF-Tu, which protrude into the GE2270A-binding site, are shown in purple stick representation. The images were created using *MOLSCRIPT* (Kraulis, 1991) and *RASTER3D* (Merritt & Bacon, 1997).

3.4. Crystal packing

Many high-resolution structures of EF-Tu complexed to various ligands have been reported. The EF-Tu–MgGDP form crystallizes easily, but many of the crystal forms have proven unsuitable for structural analysis as a consequence of poor diffraction or twinning. The present EF-Tu–MgGDP crystal form in space group $P3_121$ is reminiscent of the polymorphic crystals reported in 1976 (Leberman *et al.*, 1976), although the unit-cell parameters differ. It is not known whether the unit-cell parameters are different as a consequence of the data-collection temperature. In the present study, the unit-cell parameters are $a = b = 69.55$, $c = 169.44$ Å with a solvent content of 54.3% at 98 K, whereas in the former study the unit-cell parameters were reported to be $a = b = 80$, $c = 161$ Å with a solvent content of 63.6% for the $P3_121$ form at room temperature. In the latter report, EF-Tu–MgGDP crystallized from PEG 6000 in four different trigonal and hexagonal space groups, followed by a solid-state transition to a unique hexagonal and subsequently to another unique trigonal space group. Leberman and colleagues explained the bizarre observations by assuming a full occupancy of only one of the two molecular sites in the $P3_121$ space group. The latter investigators used precession films for partial data collection and did not have the advantage of more accurate methods to calculate the intensity distribution of the data. Given the present analysis, it appears that an alternate interpretation of the reported polymorphic crystals is the presence of various percentages of merohedral twinning. The results suggest that the present data set arose from a $P3_121$ crystal with approximately 70% of the microcrystalline domains in one orientation and another 30% in an orientation rotated parallel to *c* by 60° in order to generate the twofold twinning operator. If the microcrystalline domain percentages had been

closer to 50%, caused by a minor solution perturbation by additives, then the space group would have appeared to be $P6_222$. Similar reasoning can be applied to the other polymorphic forms of the EF-Tu–MgGDP crystals, whether grown in solution or converted in the solid state during X-ray exposure at room temperature. Although a rotational shift of 60° among microcrystalline domains in the solid state may appear to be large, the necessary rotations would be parallel with the *c* axis, in which the intermolecular contacts in the present $P3_121$ crystal form are minimal. At 95 K, there is only one contact within 3.5 Å, between Thr38 and Thr320, among the layers of molecules parallel to *c*. It is unlikely that the room-temperature $P3_121$ form, with a larger solvent content, makes more intermolecular contacts.

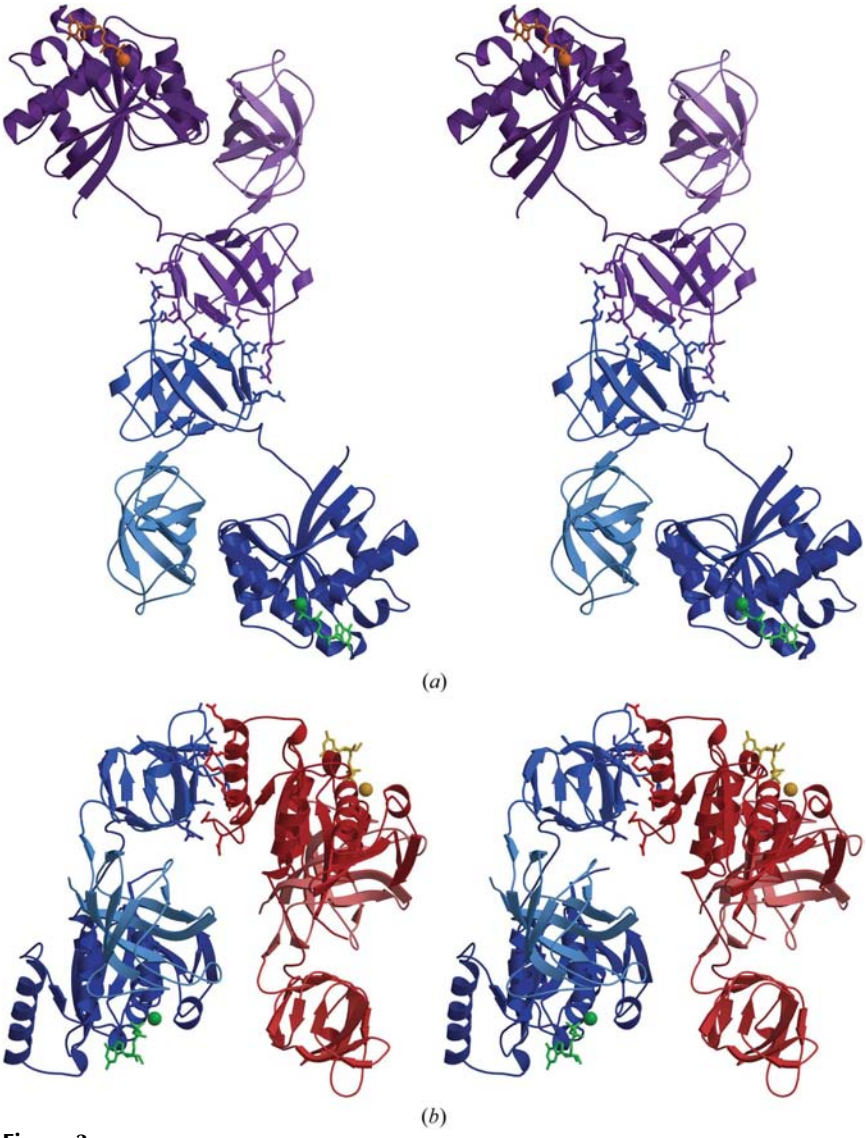

Figure 3
Stereo images of EF-Tu–MgGDP dimer interactions in the $P3_121$ crystals. One molecule of the EF-Tu dimer is shown as a blue ribbon and the symmetry-related molecule as a purple ribbon in (*a*) and as a red ribbon in (*b*). The EF-Tu molecules correspond to the Fig. 2 molecules sharing the same color. Within each molecule, the darkest hue is used for the N-terminal domain (domain 1) and the lightest hue for the C-terminal domain (domain 3). The GDP is represented by a stick model and the Mg^{2+} ion by a sphere and are colored differently in each EF-Tu molecule. The amino-acid side chains which participate in dimer interactions are shown as stick models. (*a*) The homologous dimer interactions within 3.5 Å formed between domain 2 of each EF-Tu molecule are shown. The interactions involve the side chains of residues Ser221, Arg223, Glu259, Leu264, Leu265, Asp266, Glu267, Arg269, Glu272 and Leu277 found on loops and a β-strand of each EF-Tu molecule. (*b*) The heterologous dimer interaction formed between domain 1 of EF-Tu and domain 2 of its symmetry-related neighbor is shown. The interactions within 3.5 Å are formed between residues Glu144, Glu147, Leu148, Met151, Arg154, Glu155, Gln159, Gln165 and Asp166 extended from a helix and loop in domain 1 of one EF-Tu–MgGDP molecule and residues Glu215, Asp216, Phe218, Ser219, Ile220, Ser221, Val226, Glu259, Phe261, Arg283 and Arg288 extended from a short β-strand and loops in domain 2 of the neighboring molecule. The images were created using *MOLSCRIPT* (Kraulis, 1991) and *RASTER3D* (Merritt & Bacon, 1997).

A distinctive feature of the crystal packing in the $P3_121$ form is the nature of the intermolecular EF-Tu dimers, shown in Fig. 3. Many of the liganded forms of EF-Tu exhibit dimer interactions that involve hydrogen bonding between intermolecular β strands, but the dimer interactions in the $P3_121$ crystals do not involve β-strand pairing. In general, the dimer contacts are relatively weak. One type of dimer, involving ten pairs of amino acids, is a homologous dimer formed between domain 2 of a neighboring EF-Tu–MgGDP molecule. The amino acids are located on several loops as well as on one β-strand. The second type is a heterologous dimer involving nine amino acids in domain 1 of one EF-Tu molecule and 11 amino acids from domain 2 of a neighboring molecule. The latter dimer is primarily responsible for blocking accessibility to the GE2270A-binding site.

4. Conclusions

Although twinning and mosaicity complicated the data reduction and analysis, the correct space group of the crystals has ultimately been determined to be $P3_121$ by a process of elimination throughout various stages of the structural analysis. The unit-cell parameters are $a = b = 69.55$, $c = 169.44$ Å, $\alpha = \beta = 90$, $\gamma = 120°$, resulting in a V_M of 2.7 Å Da^{-1} and a solvent content of 54.3%. The correct space-group determination resolves longstanding issues regarding polymorphic crystals of EF-Tu–MgGDP. The inhibitor compound is not present in this crystal because crystal packing occludes the binding site.

This research was supported by the National Institutes of Health (SBIR Grant to Molsoft LLC, 'Rational Design of *Yersinia pestis* EF-Tu Inhibitors'). The research was conducted in part at the

Advanced Light Source, a division of Lawrence Berkeley National Laboratory, which is operated by the University of California for and funded by the US Department of Energy. The inhibitor compound 1013-0135 was provided by Chemical Diversity Laboratories Inc. This compound was identified as a possible inhibitor of EF-Tu by Maxim Totrov of Molsoft LLC.

References

Abel, K. & Jurnak, F. (1996). *Structure*, **4**, 229–238.
Abel, K., Yoder, M. D., Hilgenfeld, R. & Jurnak, F. (1996). *Structure*, **4**, 1153–1159.
An, J., Totrov, M. & Abagyan, R. (2004). *Genome Inform. Ser. Workshop Genome Inform.* **15**, 31–41.
Anborgh, P. H., Okamura, S. & Parmeggiani, A. (2004). *Biochemistry*, **43**, 15550–15556.
Berchtold, H., Reshetnikova, L., Reiser, C. O., Schirmer, N. K., Sprinzl, M. & Hilgenfeld, R. (1993). *Nature (London)*, **365**, 126–132.
Brünger, A. T., Adams, P. D., Clore, G. M., DeLano, W. L., Gros, P., Grosse-Kunstleve, R. W., Jiang, J.-S., Kuszewski, J., Nilges, M., Pannu, N. S., Read, R. J., Rice, L. M., Simonson, T. & Warren, G. L. (1998). *Acta Cryst.* D**54**, 905–921.
Cavasotto, C. N., Orry, J. W. & Abagyan, R. A. (2003). *Proteins*, **51**, 423–433.
Cetin, R., Krab, I. M., Anborgh, P. H., Cool, R. H., Watanabe, T., Sugiyama, T., Isake, K. & Parmeggiani, A. (1996). *EMBO J.* **15**, 2604–2611.
Collaborative Computational Project, Number 4 (1994). *Acta Cryst.* D**50**, 760–763.
Deibel, M. R., Bodnar, A. L., Yem, A. W., Wolfe, C. L., Heckaman, C. L., Bohanon, M. J., Mathews, W. R., Sweeney, M. T., Zurenko, G. E., Marotti, K. R., Boyle, T. P. & Thorarensen, A. (2004). *Bioconjug. Chem.* **15**, 333–343.
Diederichs, K. & Karplus, P. A. (1997). *Nature Struct. Biol.* **4**, 269–275.
Evans, P. R. (1997). *Jnt CCP4/ESF–EACBM Newsl. Protein Crystallogr.* **33**, 22–24.
French, G. S. & Wilson, K. S. (1978). *Acta Cryst.* A**34**, 517–525.
Heffron, S. E. & Jurnak, F. (2000). *Biochemistry*, **39**, 37–45.
Jayasekera, M. M. K., Onheiber, K., Keith, J., Venkatesan, H., Santillan, A., Stocking, E. M., Tang, L., Miller, J., Gomez, L., Rhead, B., Delcamp, T., Huang, S., Wolin, R., Bobkova, E. & Shaw, K. J. (2005). *Antimicrob. Agents Chemother.* **49**, 131–136.
Jones, T. A., Bergdoll, M. & Kjeldgaard, M. (1990). *Crystallographic and Modeling Methods in Molecular Design*, edited by C. Bugg & S. Ealick, pp. 189–195. New York: Springer–Verlag.
Kawashima, T., Berthet-Colominas, C., Wulff, M., Cusack, S. & Leberman, R. (1996). *Nature (London)*, **379**, 511–518.
Kjeldgaard, M., Nissen, P., Thirup, S. & Nyborg, J. (1993). *Structure*, **1**, 35–50.
Kleywegt, G. J. & Jones, T. A. (1996). *Acta Cryst.* D**52**, 826–828.
Kraulis, P. J. (1991). *J. Appl. Cryst.* **24**, 946–950.
Laskowski, R. A., MacArthur, M. W., Moss, D. S. & Thornton, J. M. (1993). *J. Appl. Cryst.* **26**, 283–291.
Leberman, R., Wittinghofer, A. & Schulz, G. E. (1976). *J. Mol. Biol.* **106**, 951–961.
Louie, A., Ribeiro, N. S., Reid, B. R. & Jurnak, F. (1984). *J. Biol. Chem.* **259**, 5010–5016.
Merritt, E. A. & Bacon, D. J. (1997). *Methods Enzymol.* **277**, 505–524.
Nissen, P., Kjeldgaard, M., Thirup, S., Polekhina, G., Reshetnikova, L., Clark, B. F. & Nyborg, J. (1995). *Science*, **270**, 1464–1472.
Parmeggiani, A., Krab, I. M., Watanabe, T., Nielsen, R. C., Dahlberg, C., Nyborg, J. & Nissen, P. (2006). *J. Biol. Chem.* **281**, 2893–2900.
Parmeggiani, A. & Swart, G. W. M. (1985). *Annu. Rev. Microbiol.* **39**, 557–577.
Polekhina, G., Thirup, S., Kjeldgaard, M., Nissen, P., Lippmann, C. & Nyborg, J. (1996). *Structure*, **4**, 1141–1151.
Potterton, E., Briggs, P., Turkenburg, M. & Dodson, E. (2003). *Acta Cryst.* D**59**, 1131–1137.
Read, R. J. (1986). *Acta Cryst.* A**42**, 140–149.
Read, R. J. (2001). *Acta Cryst.* D**57**, 1373–1382.
Sauter, N. K., Grosse-Kunstleve, R. W. & Adams, P. D. (2004). *J. Appl. Cryst.* **37**, 399–409.
Steller, I., Bolotovsky, R. & Rossmann, M. G. (1997). *J. Appl. Cryst.* **30**, 1036–1040.
Storoni, L. C., McCoy, A. J. & Read, R. J. (2004). *Acta Cryst.* D**60**, 432–438.
Vogeley, L., Palm, G. J., Mesters, J. R. & Hilgenfeld, R. (2001). *J. Biol. Chem.* **276**, 17149–17155.
Yeates, T. O. (1997). *Methods Enzymol.* **276**, 344–358.